ACS OMEGA

http://pubs.acs.org/journal/acsodf

Article

Flavonoid Glycosides from *Ulmus macrocarpa* Inhibit Osteoclast Differentiation via the Downregulation of NFATc1

Weihong Wang,[○] Chanhyeok Jeong,[○] Yongjin Lee,[○] Chanyoon Park, Eunseok Oh, Kyu-Hyung Park, Youbin Cho, Eunmo Kang, JunI Lee, Yeon-Jin Cho, Jung Han Yoon Park, Young-Jin Son, Ki Won Lee, and Heonjoong Kang*

Cite This: *ACS Omega* 2022, 7, 4840−4849

Read Online

ACCESS | Metrics & More | Article Recommendations | Supporting Information

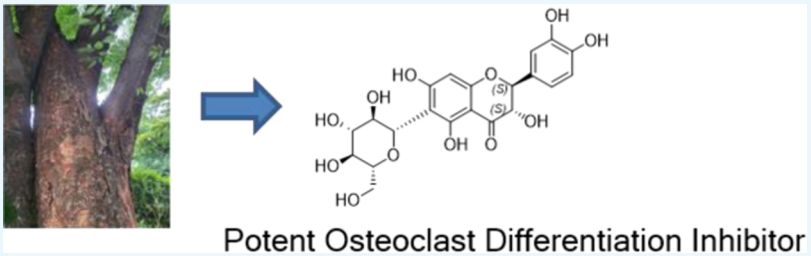

ABSTRACT: The aim of this study was to isolate and identify chemical components with osteoclast differentiation inhibitory activity from *Ulmus macrocarpa* Hance bark. Spectroscopic analyses, including nuclear magnetic resonance (NMR) and electronic circular dichroism (ECD), resulted in the unequivocal elucidation of active compounds such as (2*S*)-naringenin-6-*C*-*β*-D-glucopyranoside (**1**), (2*R*)-naringenin-6-*C*-*β*-D-glucopyranoside (**2**), (2*R*,3*S*)-catechin-7-*O*-*β*-D-xylopyranoside (**3**), (2*R*,3*S*)-catechin-7-*O*-*β*-D-apiofuranoside (**6**), (2*R*,3*R*)-taxifolin-6-*C*-*β*-D-glucopyranoside (**7**), and (2*S*,3*S*)-taxifolin-6-*C*-*β*-D-glucopyranoside (**8**). Mechanistically, the compounds may exhibit osteoclast differentiation inhibitory activity via the downregulation of NFATc1, a master regulator involved in osteoclast formation. This is the first report of their inhibitory activities on the receptor activator of nuclear factor κB ligand (RANKL)-induced osteoclast differentiation in murine bone marrow-derived macrophages. These findings provide further scientific evidence for the rational application of the genus *Ulmus* for the amelioration or treatment of osteopenic diseases.

INTRODUCTION

Bone, unlike its rigid appearance, is a dynamic organ. As much as 10% of the total bone content is replaced every year in adults. Once formed, bone undergoes a metabolic process called remodeling, which involves bone resorption by osteoclasts and bone formation by osteoblasts.[1,2] The balance between the activities of osteoclasts and osteoblasts is vital for the regulation and maintenance of the skeletal structure and function. Most adult skeletal diseases are caused by an imbalance in bone remodeling with excessive bone resorption by osteoclasts. Such osteopenic diseases would include osteoporosis, rheumatoid arthritis, periodontal disease, Paget's disease, and metastatic cancers.[1−3] Among them, osteoporosis is one of the most common chronic diseases of aging, affecting approximately 25% of women and 12.5% of men aged 50 years or older.[4] Osteoporosis seriously reduces the quality of life in patients and puts considerable strain on healthcare costs. With the rapidly growing aging population globally, osteoporosis is becoming a major public health concern. Therefore, there is an urgent need to develop effective and safe approaches for the amelioration or treatment of osteopenic diseases. Herbal medicines may be good options, owing primarily to their presumed safety, which makes them more suitable for long-term application.

Plants of the genus *Ulmus* are deciduous trees belonging to the family Ulmaceae. They consist of approximately 40 species worldwide with different species distributed in different areas.[5,6] Plants of the genus *Ulmus* are mainly located in South America, North America, Europe, Western Himalayas, and East Asia according to the phylogenic tree made by Bate-Smith.[6] Five species and one variety, *Ulmus davidiana* var. japonica (Rehder) Nakai, *Ulmus davidiana* Planch, *Ulmus macrocarpa* Hance, *Ulmus parvifolia Jacq. Nakai, Ulmus laciniata* (Trautv.) Mayr, and *Ulmus pumila* L., are found in Korea,[7,8] where the bark of the genus *Ulmus* is considered safe and has been consumed as a popular health food and folk medicine. The bark of the genus *Ulmus* can be easily found on

Received: September 24, 2021
Accepted: January 21, 2022
Published: January 31, 2022

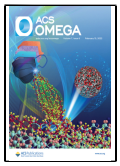

https://doi.org/10.1021/acsomega.1c05305
ACS Omega 2022, 7, 4840−4849

the internet and in markets in Korea. It has been traditionally used in Korean herbal medicine to treat gastritis, gastric cancer, rheumatoid arthritis, mastitis, hemorrhoids, jaundice, and gynecological diseases.[9−12] Recently, the crude extract of *U. davidiana* Planch was reported to inhibit bone resorption in cultured mouse osteoclasts, stimulate osteoblastic differentiation, and enhance mineralization in rat bone marrow cells.[11,13,14] Little is known about the mechanisms of action and chemical components responsible for these biological activities of *U. davidiana*, although the phytochemistry of the East Asia species has long been studied.[9,15−17]

For a long time, the bark of *U. davidiana* var. japonica (Rehder) Nakai (UD), *U. parvifolia* Jacq. Nakai, and *U. pumila* L., has been interchangeably consumed under the trivial name of yugeunpi or yubaekpi in Korea as it is very difficult to distinguish the bark of these plants from each other by the external form even for an experienced herbal pharmacist. With the improvement in plant taxonomy and medicine management, only the bark of *U. macrocarpa* Hance (UM) is currently approved as yugeunpi in the Korean herbal pharmacopoeia and food ingredients listed by the Korean Ministry of Food and Drug Safety. A literature survey revealed that the first modern pharmacological study about UM (treatment of ulcerative colitis) started in 1990,[18] 4 years earlier than its chemical studies.[9] In 2008, antihypertensive, vasorelaxant, and antioxidant effects of root bark of UM were found.[19] The responsible chemical components for the antioxidative effects were confined to phenolic compounds by another group 3 years later.[20] After that, an extract of UM was proved to prevent thrombus[21] and attenuated H_2O_2 and UVB-induced skin photoaging.[22] More recent research indicated that the extract of UM modulated lipid metabolism and improved benign prostatic hyperplasia.[23,24] Although many pharmacological studies have been carried out, it is incredible that there are only two reports on chemical studies including the first one in 1994. One of the reasons may be attributed to UD, the previous representative species of yugeunpi, which caught the most attention of chemical researchers.

The biological activities and chemical components of *U. macrocarpa* Hance were investigated as part of our continuing efforts to discover natural products that inhibit RANKL-induced osteoclast differentiation. Guided by bioassay and liquid chromatography-mass spectrometry (LC-MS) screening, six osteoclast differentiation inhibitors (**1**−**3** and **6**−**8**) were obtained along with two other structure-related analogs from the bark of *U. macrocarpa* Hance. This is the first report on the osteoclast differentiation inhibitory activity of these flavonoid glycosides. Herein, we describe the isolation, structure elucidation, and biological activities of these flavonoid glycosides.

MATERIALS AND METHODS

General Experimental Procedures. Optical rotations were measured in MeOH using a Rudolph Research Autopol III (Hackettstown, NJ). UV spectra were recorded on a Hitachi JP/U-3010 UV spectrophotometer (Tokyo, Japan). All nuclear magnetic resonance (NMR) spectra were recorded on a Bruker Ascend 700 spectrometer (Billerica Middlesex County, MA) using MeOH-d_4 (Gif-sur-Yvette, France) as a solvent. Chemical shifts were reported with reference to the respective solvent peaks (δH 3.31 and δC 49.0 for methanol-d_4). Low-resolution LC-MS data were acquired on an Agilent Technologies 1200 series HPLC coupled to an Agilent Technologies 6130 quadrupole mass spectrometer. High-resolution mass data were recorded using a TripleTOF 5600 high-resolution mass spectrometer equipped with a Quadrupole/TOF mass analyzer. All of the mass data were obtained using electron spray ionization methods. High-performance liquid chromatography (HPLC) was performed using a Waters HPLC system (Milford Worcester County, MA) equipped with a Waters 2998 photodiode array detector and a Waters 1525 binary pump. HPLC-grade solvents (Daejeon, Korea) were used for the HPLC analysis. NMR solvents were purchased from Cambridge Isotope Laboratories Inc. (Andover, MA).

Plant Material and Sample Preparation. *U. macrocarpa* Hance was purchased from the company Jinsung F.M, and its identity was confirmed by one (Ki Won Lee) of the coauthors. The bark was trimmed into small pieces and ground into a fine powder using a blender. The samples were then transferred to an appropriately labeled polypropylene zipper bag and stored at −20 °C until chemical investigation. Voucher specimens of the bark were deposited at the Laboratory of Marine Drugs in Seoul National University (# 2120006).

Isolation of Compounds. The dried *U. macrocarpa* Hance bark powder (1 kg) was extracted two times with 99.9% ethanol at room temperature. The ethanol extract (122 g) was resuspended in distilled water (500 mL) and the solution was partitioned with dichloromethane (500 mL), ethyl acetate (500 mL), and *n*-butanol (500 mL), respectively. The *n*-butanol layer was subjected to Sephadex LH-20 size exclusion chromatography and eluted with methanol to afford 46 fractions (UMB1−UMB46). Fractions UMB7 and UMB8 contained similar chemical components. A combination (2.4 g) of UMB7 and UMB8 was applied to reversed-phase flash column chromatography (10 × 15 cm^2, C-18, 60 Å, 500/400 mesh, SILICYCLE, Canada) and eluted with a step gradient solvent system of 10−45% MeOH/H_2O (800 mL/fraction). Overall, 16 subfractions (UMB78-1−UMB78-16) were acquired. Compounds **1** (25 mg) and **2** (14 mg) were obtained at the retention time (RT) of 22 and 23 min, respectively, by purification of subfraction UMB78-9 on an RP column (Synersi Fusion-C18, 250 × 10 mm^2, 4 μm, 80 Å) eluting with 30% MeOH. Subfraction UMB78-3 was further purified to give compounds **3** (TR: 24 min; 12 mg), **7** (TR: 16 min; 31 mg), and **8** (TR: 18 min; 19 mg) using the same column eluting with 20% MeOH. The separation of fraction UMB6 on reversed-phase (RP) HPLC equipped with a Phenomenex Luna C18 column (5 μm, 100 Å, 250 × 100 mm^2) yielded compound **4** (TR: 21 min; 33 mg) by elution with 35% methanol. Fractions UMB9−UMB12 were combined due to their similar chemical components and chromatographed on the abovementioned flash column with step gradient elution (from 20 to 50% MeOH) to give 10 subfractions (UMB912-1−UMB912-10). Compound **5** (RT: 25 min; 34 mg) was obtained by separation of UMB912-7 using RP HPLC (Phenomenex Luna C18, 5 μm, 100 Å, 250 × 100 mm^2) eluted with 40% MeOH. Purification of UMB912-3 gave compound **6** (29 mg) at a retention time of 27 min on the same RP HPLC column eluted with 25% MeOH.

*(2S)-Naringenin-6-C-β-D-glucopyranoside (**1**).* White amorphous powder; $[\alpha]_D^{20}$ +18.6 (*c* 0.20, MeOH); UV (MeOH) λ_{max} 220, 291, 330; electronic circular dichroism (ECD) (1.2 × 10^{-3} M, MeOH) λ_{max} ($\Delta\varepsilon$) 289 nm (−6.09), 217 nm (+6.92); ^{1}H NMR (methanol-d_4, 700 MHz) δ 7.30 (d, J = 8.5 Hz, H-2′/6′), 6.81 (d, J = 8.5 Hz, H-3′/5′), 5.94 (s, H-

https://doi.org/10.1021/acsomega.1c05305
ACS Omega 2022, 7, 4840−4849

8), 5.34 (dd, J = 12.6, 2.9 Hz, H-2), 4.79 (d, J = 9.9 Hz, H-1″), 4.14 (t, J = 9.9 Hz, H-2″), 3.85 (dd, J = 12.1, 2.2 Hz, H-6″a), 3.71 (dd, J = 12.1, 5.5 Hz, H-6″b), 3.44 (m, H-4′′), 3.43 (m, H-3′′), 3.37 (m, H-5′′), 3.11 (dd, J = 17.1, 12.6 Hz, H-3a), 2.73 (dd, J = 17.1, 3.1 Hz, H-3b); ^{13}C NMR (methanol-d_4, 175 MHz) δ 197.7 (C-4), 168.6 (C-7), 164.4 (C-5), 164.2 (C-9), 159.0 (C-4′), 131.0 (C-1′), 129.0 (C-2′/6′), 116.3 (C-3′/5′), 106.1 (C-6), 103.0 (C-10), 96.7 (C-8), 82.5 (C-5″), 80.4 (C-2), 80.3 (C-3′′), 75.3 (C-1′′), 72.6 (C-2′′), 71.8 (C-4′′), 62.9 (C-6′′), 43.9 (C-3); ESIMS m/z 435 $[M + H]^+$, 433 $[M - H]^-$; HRESIMS m/z 435.1281 $[M + H]^+$ (calcd for $C_{21}H_{23}O_{10}$, 435.1291).

(2R)-Naringenin-6-C-β-D-glucopyranoside (**2**). White amorphous powder; $[\alpha]_D^{20}$ +13.8 (c 0.50, MeOH); UV (MeOH) λ_{max} 220, 291, 330; ECD (0.9 × 10^{-3} M, MeOH) λ_{max} ($\Delta\varepsilon$) 290 nm (+5.48), 216 nm (−6.91); ^{1}H NMR (methanol-d_4, 700 MHz) δ 7.30 (d, J = 8.6 Hz, H-2′/6′), 6.81 (d, J = 8.6 Hz, H-3′/5′), 5.89 (s, H-8), 5.33 (dd, J = 12.6, 3.0 Hz, H-2), 4.78 (d, J = 9.9 Hz, H-1″), 4.19 (t, J = 9.9 Hz, H-2″), 3.84 (dd, J = 12.1, 2.0 Hz, H-6″a), 3.71 (dd, J = 12.1, 5.7 Hz, H-6″b), 3.46 (m, H-4′′), 3.43 (m, H-3′′), 3.37 (m, H-5′′), 3.08 (dd, J = 17.1, 12.6 Hz, H-3a), 2.71 (dd, J = 17.1, 3.1 Hz, H-3b); ^{13}C NMR (methanol-d_4, 175 MHz) δ 196.8 (C-4), 170.9 (C-7), 164.5 (C-5), 164.1 (C-9), 159.0 (C-4′), 131.2 (C-1′), 129.0 (C-2′/6′), 116.3 (C-3′/5′), 106.4 (C-6), 102.3 (C-10), 97.5 (C-8), 82.4 (C-5″), 80.4 (C-3′′), 80.1 (C-2), 75.4 (C-1′′), 72.3 (C-2′′), 71.8 (C-4′′), 62.9 (C-6′′), 43.8 (C-3); ESIMS m/z 435 $[M + H]^+$, 433 $[M - H]^-$; HRESIMS m/z 435.1278 $[M + H]^+$ (calcd for $C_{21}H_{23}O_{10}$, 435.1291).

(2R,3S)-Catechin-7-O-β-D-xylopyranoside (**3**). White amorphous powder; $[\alpha]_D^{20}$ −15.6 (c 0.50, MeOH); UV (MeOH) λ_{max} 203, 279; ECD (2.6 × 10^{-3} M, MeOH) λ_{max} ($\Delta\varepsilon$) 276 nm (−1.33), 215 nm (−5.06); ^{1}H NMR (methanol-d_4, 700 MHz) δ 6.83 (d, J = 1.8 Hz, H-2′), 6.76 (d, J = 8.1 Hz, H-5′), 6.72 (dd, J = 8.1, 1.8 Hz, H-6′), 6.17 (d, J = 2.2 Hz, H-6), 6.11 (d, J = 2.2 Hz, H-8), 4.76 (d, J = 7.1 Hz, H-1″), 4.60 (d, J = 7.4 Hz, H-2), 4.00 (m, H-3), 3.90 (dd, J = 11.5, 5.4 Hz, H-5″a), 3.54 (m, H-4′′), 3.39 (m, H-3′′), 3.38 (m, H-2′′), 3.32 (overlapped with solvent peaks, H-5′′b), 2.86 (dd, J = 16.3, 5.4 Hz, H-3a), 2.54 (dd, J = 16.3, 8.0 Hz, H-3b); ^{13}C NMR (methanol-d_4, 175 MHz) δ 158.5 (C-7), 157.6 (C-5), 156.8 (C-9), 146.29 (C-4′), 146.26 (C-3′), 132.1 (C-1′), 120.0 (C-6′), 116.1 (C-5′), 115.2 (C-2′), 103.7 (C-10), 102.9 (C-1″), 97.4 (C-6), 97.0 (C-8), 82.9 (C-2), 77.8 (C-3′′), 74.7 (C-2′′), 71.0 (C-4′′), 68.6 (C-3), 66.9 (C-5′′), 28.5 (C-4); ESIMS m/z 423 $[M + H]^+$, 421 $[M - H]^-$; HRESIMS m/z 423.1278 $[M + H]^+$ (calcd for $C_{20}H_{23}O_{10}$, 423.1291).

(2R,3R)-Aromadendrin-6-C-β-D-glucopyranoside (**4**). White amorphous powder; $[\alpha]_D^{20}$ +34.1 (c 0.50, MeOH); UV (MeOH) λ_{max} (log ε) 197, 226, 294, 330; ECD (1.2 × 10^{-3} M, MeOH) λ_{max} ($\Delta\varepsilon$) 293 nm (−7.45), 256 nm (+1.25), 235 nm (+2.85), 217 nm (+9.62); ^{1}H NMR (methanol-d_4, 700 MHz) δ 7.34 (d, J = 8.5 Hz, H-2′/6′), 6.83 (d, J = 8.5 Hz, H-3′/5′), 5.92 (s, H-8), 4.97 (d, J = 11.4 Hz, H-2), 4.79 (d, J = 9.9 Hz, H-1″), 4.53 (d, J = 11.4 Hz, H-3), 4.14 (t, J = 9.1 Hz, H-2″), 3.85 (dd, J = 12.1, 2.2 Hz, H-6″a), 3.71 (dd, J = 12.1, 5.5 Hz, H-6″b), 3.45 (m, H-4′′), 3.44 (m, H-3′′), 3.37 (m, H-5′′); ^{13}C NMR (methanol-d_4, 175 MHz) δ 198.3 (C-4), 169.3 (C-7), 164.2 (C-5), 163.8 (C-9), 159.0 (C-4′), 130.3 (C-1′), 129.3 (C-2′/6′), 116.2 (C-3′/5′), 106.5 (C-6), 101.3 (C-10), 96.9 (C-8), 84.9 (C-2), 82.5 (C-5″), 80.3 (C-3′′), 75.2 (C-1′′), 73.6 (C-3), 72.5 (C-2′′), 71.8 (C-4′′), 62.9 (C-6′′); ESIMS m/z 451 $[M + H]^+$, 449 $[M - H]^-$; HRESIMS m/z 451.1229 $[M + H]^+$ (calcd for $C_{21}H_{23}O_{11}$, 451.1240).

Kaempferol 6-C-β-D-Glucopyranoside (**5**). White amorphous powder; UV (MeOH) λ_{max} (log ε) 198, 269, 368; ^{1}H NMR (methanol-d_4, 700 MHz) δ 8.08 (d, J = 8.5 Hz, H-2′/6′), 6.90 (d, J = 8.5 Hz, H-3′/5′), 6.45 (s, H-8), 4.91 (d, J = 9.9 Hz, H-1″), 4.19 (t, J = 9.9 Hz, H-2″), 3.88 (dd, J = 12.2, 2.2 Hz, H-6″a), 3.74 (dd, J = 12.2, 5.4 Hz, H-6″b), 3.48 (m, H-4′′), 3.48 (m, H-3′′), 3.42 (m, H-5′′); ^{13}C NMR (methanol-d_4, 175 MHz) δ 177.5(C-4), 164.9 (C-7), 161.3 (C-5), 160.6 (C-4′), 157.6 (C-9), 148.0 (C-2), 137.2 (C-3), 130.2 (C-2′/6′), 123.6 (C-1′), 116.0 (C-3′/5′), 108.4 (C-6), 104.4 (C-10), 95.3 (C-8), 83.0 (C-5″), 80.6 (C-3′′), 75.7 (C-1′′), 72.9 (C-2′′), 72.2 (C-4′′), 62.9 (C-6′′); ESIMS m/z 449 $[M + H]^+$, 447 $[M - H]^-$; HRESIMS m/z 449.1075 $[M + H]^+$ (calcd for $C_{21}H_{21}O_{11}$, 449.1084).

(2R,3S)-Catechin-7-O-β-D-apiofuranoside (**6**). White amorphous powder; $[\alpha]_D^{20}$ −90.7 (c 0.50, MeOH); UV (MeOH) λ_{max} 203, 280; ECD (1.9 × 10^{-3} M, MeOH) λ_{max} ($\Delta\varepsilon$) 276 nm (−1.16), 212 nm (−5.95); ^{1}H NMR (methanol-d_4, 700 MHz) δ 6.83 (d, J = 1.9 Hz, H-2′), 6.76 (d, J = 8.1 Hz, H-5′), 6.71 (dd, J = 8.1, 1.9 Hz, H-6′), 6.13 (d, J = 2.3 Hz, H-6), 6.07 (d, J = 2.3 Hz, H-8), 5.48 (d, J = 2.9 Hz, H-1″), 4.60 (d, J = 7.4 Hz, H-2), 4.13 (d, J = 2.9 Hz, H-2″), 4.08 (d, J = 9.7 Hz, H-4″a), 3.99 (m, H-3), 3.84 (d, J = 9.7 Hz, H-4″b), 3.62 (d, J = 11.4 Hz, H-5″a), 3.59 (d, J = 11.4 Hz, H-5″b), 2.85 (dd, J = 16.3, 5.5 Hz, H-3a), 2.54 (dd, J = 16.3, 8.0 Hz, H-3b); ^{13}C NMR (methanol-d_4, 175 MHz) δ 158.2 (C-7), 157.6 (C-5), 156.9 (C-9), 146.27 (C-4′), 146.25 (C-3′), 132.1 (C-1′), 120.0 (C-6′), 116.1 (C-5′), 115.2 (C-2′), 108.7 (C-1″), 103.2 (C-10), 97.3 (C-6), 96.9 (C-8), 82.9 (C-2), 80.3 (C-3′′), 78.3 (C-2′′), 75.4 (C-4′′), 68.6 (C-3), 64.9 (C-5′′), 28.4 (C-4); ESIMS m/z 423 $[M + H]^+$, 421 $[M - H]^-$; HRESIMS m/z 423.1275 $[M + H]^+$ (calcd for $C_{21}H_{23}O_{10}$, 423.1291).

(2R,3R)-Taxifolin-6-C-β-D-glucopyranoside (**7**). White amorphous powder; $[\alpha]_D^{20}$ +17.3 (c 0.50, MeOH); UV (MeOH) λ_{max} 200, 221, 290, 332; ECD (2.8 × 10^{-3} M, MeOH) λ_{max} ($\Delta\varepsilon$) 333 nm (+2.20), 297 nm (−6.98), 218 nm (+7.99); ^{1}H NMR (methanol-d_4, 700 MHz) δ 6.95 (d, J = 1.9 Hz, H-2′), 6.84 (d, J = 8.1 Hz, H-5′), 6.80 (dd, J = 8.1, 1.9 Hz, H-6′), 5.93 (s, H-8), 4.92 (d, J = 11.3 Hz, H-2), 4.80 (d, J = 9.9 Hz, H-1″), 4.50 (d, J = 11.3 Hz, H-3), 4.14 (t, J = 8.8 Hz, H-2″), 3.86 (dd, J = 12.1, 2.2 Hz, H-6″a), 3.71 (dd, J = 12.1, 5.5 Hz, H-6″b), 3.44 (m, H-4′′), 3.43 (m, H-3′′), 3.38 (m, H-5′′); ^{13}C NMR (methanol-d_4, 175 MHz) δ 198.4 (C-4), 168.6 (C-7), 164.2 (C-5), 163.8 (C-9), 147.2 (C-4′), 146.3 (C-3′), 129.8 (C-1′), 120.4 (C-6′), 116.1 (C-5′), 115.8 (C-2′), 106.4 (C-6), 101.5 (C-10), 96.7 (C-8), 85.1 (C-2), 82.5 (C-5″), 80.2 (C-3′′), 75.2 (C-1′′), 73.6 (C-3), 72.6 (C-2′′), 71.8 (C-4′′), 62.9 (C-6′′); ESIMS m/z 467 $[M + H]^+$, 465 $[M - H]^-$; HRESIMS m/z 467.1183 $[M + H]^+$ (calcd for $C_{21}H_{23}O_{12}$, 467.1190).

(2S,3S)-Taxifolin-6-C-β-D-glucopyranoside (**8**). White amorphous powder; $[\alpha]_D^{20}$ −7.3 (c 0.50, MeOH); UV (MeOH) λ_{max} 200, 221, 290, 332; ECD (2.1 × 10^{-3} M, MeOH) λ_{max} ($\Delta\varepsilon$) 331 nm (−0.67), 297 nm (+4.65), 227 nm (−6.82), 206 nm (−6.23); ^{1}H NMR (methanol-d_4, 700 MHz) δ 6.95 (d, J = 1.9 Hz, H-2′), 6.84 (d, J = 8.1 Hz, H-5′), 6.80 (dd, J = 8.1, 1.9 Hz, H-6′), 5.95 (s, H-8), 4.93 (d, J = 11.3 Hz, H-2), 4.80 (d, J = 9.9 Hz, H-1″), 4.50 (d, J = 11.3 Hz, H-3), 4.13 (t, J = 8.8 Hz, H-2″), 3.86 (dd, J = 12.1, 2.2 Hz, H-6″a), 3.71 (dd, J = 12.1, 5.5 Hz, H-6″b), 3.44 (m, H-4′′), 3.43 (m, H-3′′), 3.38 (m, H-5′′); ^{13}C NMR (methanol-d_4, 175 MHz) δ

https://doi.org/10.1021/acsomega.1c05305
ACS Omega 2022, 7, 4840−4849

Table 1. Primer Sequences Used in This Study

gene of interest	primer sequence (5′ → 3′)	
	sense	antisense
NFATc1	GGGTCAGTGTGACCGAAGAT	GGAAGTCAGAAGTGGGTGGA
CTSK	GGCCAACTCAAGAAGAAAAC	GTGCTTGCTTCCCTTCTGG
OSCAR	CTGCTGGTAACGGATCAGCTC	CCAAGGAGCCAGAACCTT
DC-STAMP CCAAGGAGTCGTCCATGATT	GGCTGCTTTGATCGTTTCTC	
GAPDH	AACTTTGGCATTGTGGAAGG	ACACATTGGGGGTAGGAACA

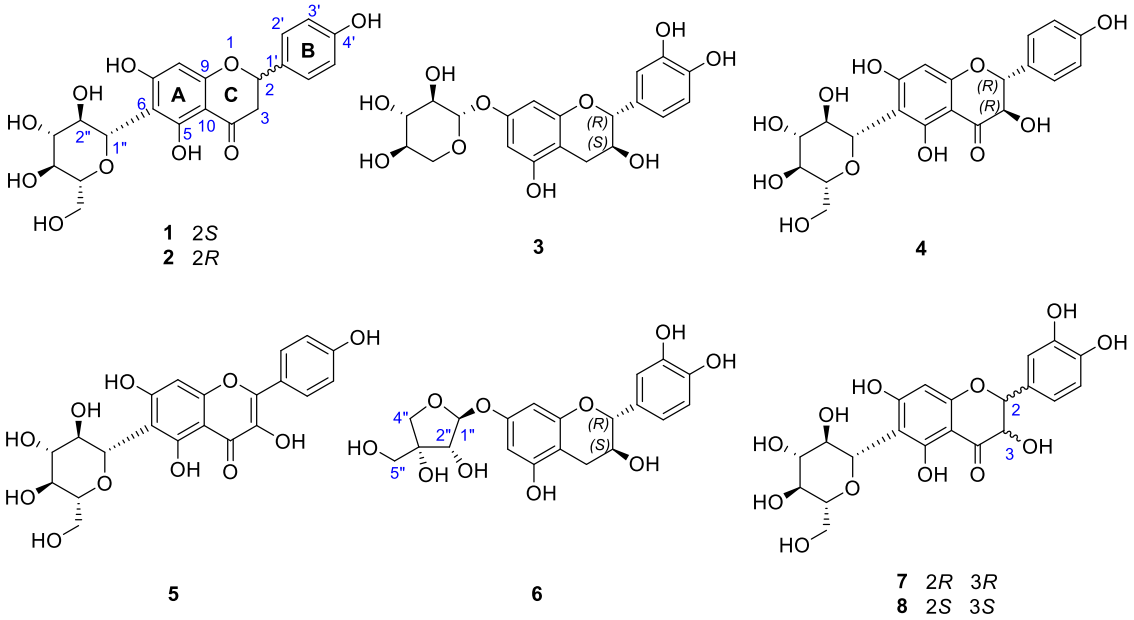

Figure 1. Chemical structures of compounds **1**−**8**.

198.7 (C-4), 167.9 (C-7), 164.1 (C-5), 163.8 (C-9), 147.2 (C-4′), 146.3 (C-3′), 129.7 (C-1′), 120.8 (C-6′), 116.1 (C-5′), 115.9 (C-2′), 106.3 (C-6), 101.7 (C-10), 96.5 (C-8), 85.0 (C-2), 82.5 (C-5″), 80.2 (C-3″), 75.2 (C-1″), 73.6 (C-3), 72.5 (C-2″), 71.8 (C-4″), 62.9 (C-6″); ESIMS m/z 467 $[M + H]^+$, 465 $[M - H]^-$; HRESIMS m/z 467.1174 $[M + H]^+$ (calcd for $C_{21}H_{23}O_{12}$, 467.1190).

Osteoclast Differentiation and Tartrate-Resistant Acid Phosphatase (TRAP) Staining. Osteoclast differentiation and TRAP staining were carried out as previously reported.[25] Bone marrow cells (BMCs) were isolated in strict accordance with the Standard Protocol for Animal Study of Sunchon National University (SCNU). The animal use protocol was approved by the Institutional Animal Care and Use Committee of SCNU (Permit No. SCNU IACUC 2021-05). All efforts were made to minimize suffering. In short, bone marrow cells (BMCs) were isolated by flushing femurs and tibias of 5-week-old ICR mice.[25] The isolated BMCs were cultured in α-MEM supplemented with 10% fetal bovine serum (FBS) (Invitrogen Life Technologies, Grand Island, NY) with 10 ng/mL M-CSF (R&D Systems) for 1 day. Bone marrow macrophages, obtained by removing floating cells, were used for osteoclast differentiation. BMMs (1×10^4 cells/well) were cultured with M-CSF (30 ng/mL) and RANKL (10 ng/mL; R&D Systems) for 3 days to generate preosteoclasts. The preosteoclasts were treated with vehicle or indicated compounds in the presence of M-CSF (30 ng/mL) for 30 min and then cultured with RANKL (10 ng/mL) to differentiate into mature tartrate-resistant acid phosphatase-positive multinucleated cells (TRAP$^+$-MNCs). After 1 day, the cells were fixed with 3.7% formaldehyde for 5 min, permeabilized with 0.1% Triton X-100 for 5 min, and stained using the leukocyte acid phosphatase kit 387-A.

Cell Viability Assay. Cell viability was assessed after 72 h of treatment with only vehicle or indicated compounds by assessing the conversion of WST-8 [2-(2-methoxy-4-nitrophenyl)-3-(4-nitrophenyl)-5-(2,4-disulfophenyl)-2*H*-tetrazolium, monosodium salt] to formazan according to the manufacturer's instructions (Dojindo, Kumamoto, Japan). The isolated BMMs (1×10^4 cells/well) were incubated in the presence of M-CSF (30 ng/mL) in 96-well plates for 12 h, and then each well was treated with dimethyl sulfoxide (DMSO) or flavonoid compounds at the indicated concentrations. After 3 days, 10 μL of a WST-8 solution was added to each well, and the plates were incubated for 4 h at 37 °C. The optical density was measured at 450 nm using a standard microplate reader (Thermo, Varioskan Flash, U.K.).

Real-Time Polymerase Chain Reaction (PCR). Real-time PCR was performed as previously described.[26] BMMs were incubated with M-CSF (30 ng/mL) in 10% FBS α-MEM and activated with RANKL (10 ng/mL) for 0, 1, 2, or 3 days in the presence of compound **8**. PCR primer sets (Table 1) were designed using the online Primer3 program.[27] Total RNA was isolated using a TRIzol reagent (Thermo Fisher Scientific Inc., Waltham, MA), and cDNA was synthesized using the M-MLV cDNA synthesis kit (Enzynomics, Daejeon, Korea). PCR was performed using a TOPreal qPCR 2x PreMIX (Bio-Rad, Hercules, CA) in a real-time PCR detection system (Bio-Rad).

https://doi.org/10.1021/acsomega.1c05305
ACS Omega 2022, 7, 4840−4849

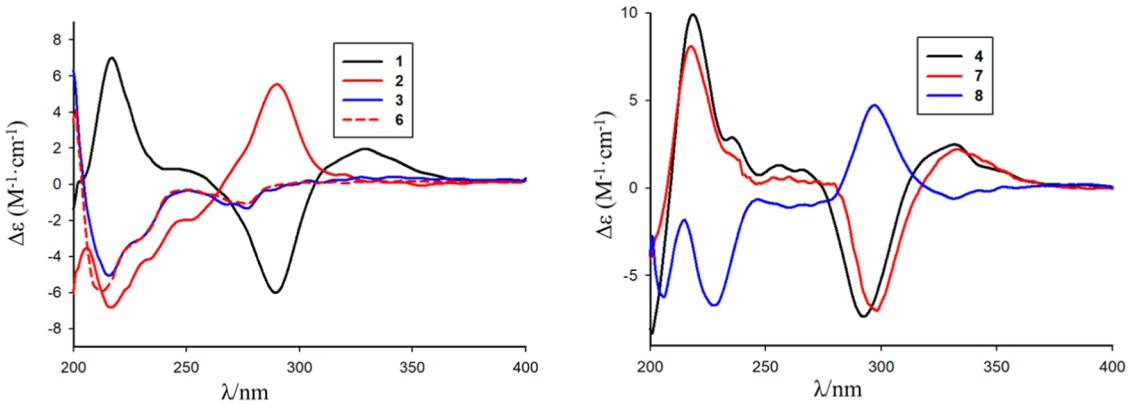

Figure 2. Electronic circular dichroism (ECD) spectra of compounds **1**−**3** and **6**−**8**.

The mRNA levels of the genes were determined using the $2^{-\Delta\Delta C_T}$ method. Glyceraldehyde-3-phosphate dehydrogenase (GAPDH) was used as an internal standard.

Western Blotting. Western blotting analysis was performed as previously described.[26] Briefly, BMMs were incubated with RANKL (10 ng/mL) and M-CSF (30 ng/mL) in 10% FBS α-MEM for 0, 1, 2, or 3 days in the presence of compound **8**. Harvested cells were lysed in lysis buffer containing protease inhibitors and quantified using the Bradford assay. Isolated proteins were separated using 10% sodium dodecyl sulfate-polyacrylamide gel electrophoresis (SDS-PAGE) and transferred to a poly(vinylidene difluoride) (PVDF) membrane (Millipore). The membrane was incubated with a primary antibody (NFATc1) at 4 °C overnight. β-actin was used for the loading control.

Statistical Analysis. Results are expressed as mean ± standard deviation (SD) of three replicates. Statistical differences were analyzed using Student's *t*-test. Probability values lower than 0.05 were considered significant (*P* values * < 0.05, ** < 0.01, *** < 0.001).

RESULTS AND DISCUSSION

Structure Elucidation of Active Compounds. The ethanolic extract of *U. macrocarpa* Hance bark demonstrated a significant inhibitory effect on osteoclast differentiation at initial screening. Solvent partition of the extract followed by repeated chromatography led to the isolation of eight flavonoid glycosides, including six osteoclast differentiation inhibitors (Figure 1).

Active compound **1** showed UV absorption at 220 nm (maximum), 291 nm (maximum), and 330 nm (inflection), which is reminiscent of a flavanone structure. Positive and negative electrospray ionization (ESI) MS gave protonated molecular ion peaks at *m/z* 435 $[M + H]^+$ and 433 $[M - H]^-$, respectively. In the ^{1}H NMR spectrum, compound **1** exhibited an aromatic singlet at δ 5.94 for H-8 of a 1,2,3,4,5-pentasubstituted benzene ring and two aromatic doublets at δ 7.30 for H-2′/6′ and δ 6.81 for H-3′/5′ of a para-disubstituted benzene ring. In addition, three coupling aliphatic protons were observed at δ 5.34, 3.11, and 2.73, which can be assigned to H-2, H-3a, and H-3b, respectively, suggesting a naringenin aglycone. In addition to the signals ascribed to flavanone aglycone, the ^{1}H NMR spectrum also showed seven aliphatic oxygenated proton signals expected for a hexose unit. Examination of the coupling constants of the sugar part, especially the coupling constant of 9.9 Hz observed between H-1″ and H-2″, and comparing these values with those reported for β-D-glucopyranosides and α-D-glucopyranosides,[28−30] the D-glucopyranose moiety and the β-configuration were unequivocally identified. The 6-*C*-linkage of the glucose moiety was confirmed by the characteristic ^{13}C chemical shift of C-1″ at δ 75.3 and the HMBC correlations from H-1′′ to its neighboring carbon atoms C-5, C-6, and C-7.

The active compound **2** was well differentiated from compound **1** in our achiral HPLC separation but exhibited exactly the same UV and MS spectra and very similar NMR spectra to compound **1**, which resulted in the assignment of a β-D-glucopyranose unit and an aglycone with the same atomic connection as **1**. The absolute configuration at C-2 was assessed by ECD spectroscopy because flavonoid glycosides show Cotton effects (CEs) quite similar to their optically active aglycones.[31] Compound **1** displayed a negative CE, while compound **2** exhibited a positive CE in the $\pi \rightarrow \pi^*$ region at 290 nm, which established the 2*S* and 2*R* configuration for compounds **1** and 2, respectively, in accordance with the modified octant rule.[32] Thus, compounds **1** and **2** were determined as (2*S*)- and (2*R*)-naringenin-6-*C*-β-D-glucopyranoside, respectively (Figure 2).

Active compounds **3** and **6** share the same flavan-3-ol aglycone and differ only in the sugar moiety. The presence of β-D-xylopyranose in compound **3** and β-D-apiofuranose in compound **6** was indicated by the chemical shifts and coupling constants including those typical for the anomeric atoms [δ 4.76 (J = 7.1 Hz) for H-1″ and δ 102.9 for C-1″ in **3**; δ 5.48 (J = 2.9 Hz) for H-1″ and δ 108.7 for C-1″ in **6**]. The 2,3-*trans* relative configuration of the aglycone moiety was confirmed by the vicinal coupling constant of H-2−H-3 (7.4 Hz). A small value of less than 2 Hz, often appearing as a broad singlet, was reported for a 2,3-*cis* configured flavan-3-ol.[33] Flavan-3-ols with a 2*R* configuration gave rise to a negative CE at around 280 nm (^{1}Lb transition), which is irrelevant to the configuration at C-3.[34−36] Accordingly, the 2*R*,3*S* absolute configuration was corroborated for compounds **3** and **6** based on the negative CE at 276 nm.

As in the case of **1** and **2**, active compounds **7** and **8** displayed a different elution order in the achiral HPLC system but the same UV and MS and almost the same NMR spectra. Compound **7** showed UV absorption at 200, 221, 290, and 332 nm, and the positive and negative ion ESIMS gave protonated molecular ion peaks at m/z 467 $[M + H]^+$ and 465 $[M - H]^-$, respectively, 32 amu more than the corresponding ion peaks of compound **1**. In addition to the proton signals assigned to a β-

https://doi.org/10.1021/acsomega.1c05305
ACS Omega 2022, 7, 4840−4849

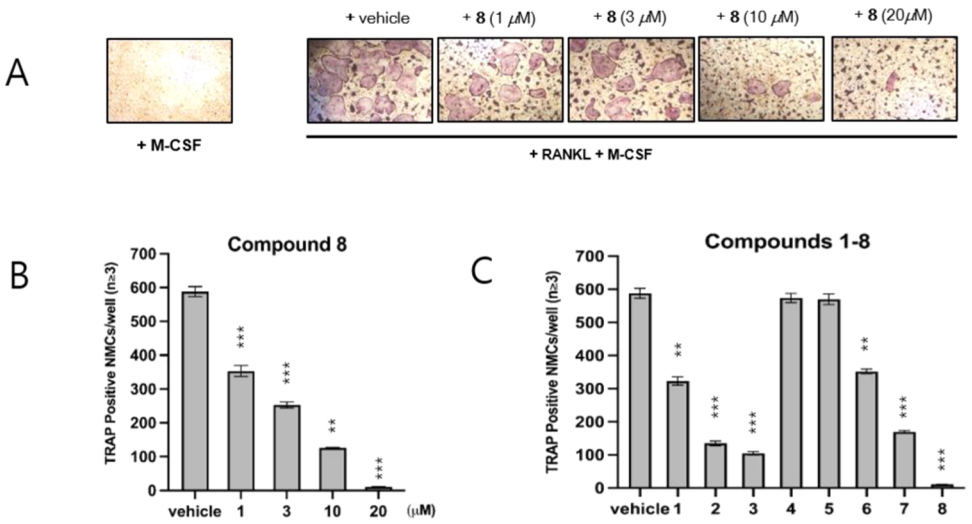

Figure 3. (A, B) Effects of compound **8** on RANKL-induced osteoclast differentiation at the concentrations of 1, 3, 10, and 20 μM. Bone marrow-derived macrophages were cultured for 4 days with M-CSF (30 ng/mL) and RANKL (10 ng/mL) in the presence of DMSO or indicated concentrations of compounds. The cells were fixed, permeabilized, and stained with a TRAP solution. Mature TRAP-positive multinucleated osteoclasts were photographed under a light microscope. TRAP-positive cells were counted as osteoclasts (nuclei $\geq$ 3). (C) Effects of compounds **1**−**8** on RANKL-induced osteoclast differentiation at a concentration of 20 μM; *P < 0.05, **P < 0.01, ***P < 0.001.

D-glucopyranose part and an aromatic singlet for H-8 at δ 5.93, the ^{1}H NMR spectrum of compound **7** showed three additional aromatic protons at δ 6.95, 6.84, and 6.80 derived from a 1,2,4-trisubstituted phenol ring and two coupling oxygenated methines at δ 4.92 (H-2) and 4.50 (H-3), suggesting the presence of two additional hydroxyl groups in **7** compared to **1**. The 2,3-*trans* relative configuration was revealed by the large $J_{2,3}$ coupling constant of 11.3 Hz. Compounds **7** and **8** differed from each other only in the absolute configuration at C-2 and C-3. The absolute configuration at C-2 was defined by the characteristic CEs. A negative $\pi \rightarrow \pi^*$ CE at 296 nm and a positive $n \rightarrow \pi^*$ CE at 333 nm were observed for compound **7**, while compound **8** exhibited opposite signs in the two regions with a positive $\pi \rightarrow \pi^*$ CE at 297 nm and a negative n $\rightarrow \pi^*$ CE at 331 nm. Hence, 2*R* for **7** and 2*S* for **8** were established.[35] Finally, compounds **7** and **8** were elucidated as (2*R*,3*R*)- and (2*S*,3*S*)-taxifolin-6-*C*-β-D-glucopyranoside, respectively.

Compounds **4** and **5** were identified as (2*R*,3*R*)-aromadendrin-6-*C*-β-D-glucopyranoside and kaempferol 6-*C*-glucopyranoside, respectively, using the same strategy as the above-mentioned active compounds. The present study, for the first time, reported the isolation of compounds **1**−**5** and **8** from *U. macrocarpa* Hance and provided an unambiguous assignment of the structure of compounds **2**, **4**, and **7** by a combination of NMR and MS techniques.

Flavonoids are an important class of valuable secondary metabolites found in plants and are commonly consumed as food and pharmaceutical materials. Based on the structural modification of ring C including the oxidation state, flavonoids can be divided into several subclasses, including flavanone, flavanonol, flavan, and flavonol. In addition, the variety of structures is known to be derived from the modification of the C6−C3−C6 skeleton by hydroxylation, glycosylation, methoxylation, as well as other modifications, and combinations thereof. The present study reported two flavanones (**1** and **2**), three flavanonols (**4**, **7**, and **8**), two flavans (**3** and **6**), and one flavonol (**5**). Among them, diastereoisomers **1** and **2** were obtained in a 3:1 ratio and diastereoisomers **7** and **8** were isolated in a 4:1 ratio. Both pairs of diastereoisomers were for the first time found to co-occur in the genus *Ulmus*, but it is unsurprising given that flavonoid enantiomers have been characterized in free form or bonded to glycosides in some other plants.[37−40] Identification and determination of these diastereoisomers will allow for the selection of a specific pharmaceutical application since most enzymatic reactions acquire high stereoselectivity.

Osteoclast Differentiation Inhibitory Activity of Isolated Compounds. Mature osteoclasts originate from bone marrow-derived macrophages (BMMs). The differentiation and proliferation of BMMs are mainly regulated by the receptor activator of nuclear factor (NF)-κB ligand (RANKL) and macrophage colony-stimulating factor 1 (M-CSF).[1,41,42] Thus, the RANKL signaling pathway is often employed as a promising target for suppressing excessive osteoclast differentiation characteristic of a variety of bone diseases including osteoporosis.

To examine the inhibitory activity of these flavonoid glycosides on RANKL-induced osteoclast differentiation, BMMs were incubated with 10 ng/mL RANKL and 30 ng/mL M-CSF for 3 days to generate preosteoclasts, which were treated with vehicle or indicated compounds in the presence of M-CSF (30 ng/mL) for 30 min and cultured with RANKL (10 ng/mL) for another day to differentiate into mature tartrate-resistant acid phosphatase-positive multinucleated osteoclast cells (TRAP$^+$-MNCs). TRAP was employed as a primary marker since it was reported to be highly expressed in osteoclasts. As shown in Figure 3C, compounds **2**, **3**, **7**, and **8** exhibited potent inhibitory activity on RANKL-induced osteoclast differentiation of BMMs into mature osteoclasts, while compounds **1** and **6** were weakly active and compounds **4** and **5** were inactive in the present study. Compounds **2**, **3**, **7**, and **8** suppressed RANKL-induced differentiation of BMMs by 77, 82, 65, and 97%, respectively, at a concentration of 20 μM (Figure S1). The test concentration of the most potent compound **8** was extended to 1 μM, and compound **8** suppressed RANKL-induced osteoclast differentiation in a dose-dependent manner (Figure 3B). None of the test

https://doi.org/10.1021/acsomega.1c05305
ACS Omega 2022, 7, 4840−4849

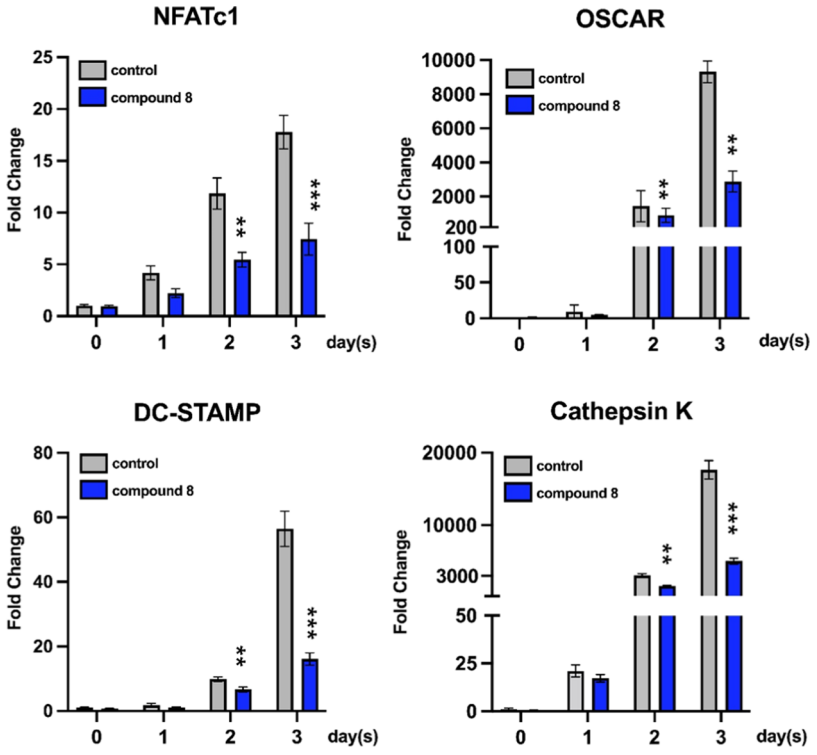

Figure 4. Effects of compound **8** (20 μM) on the RANKL-induced mRNA expression of osteoclast differentiation-specific genes. Effects of compound **8** on RANKL-mediated NFATc1, DC-STAMP, OSCAR, and CTSK expressions were analyzed by real-time PCR over a 3 day period. Con: DMSO. *P < 0.05; **P < 0.01; ***P < 0.001.

compounds showed any significant cytotoxic effects on BMMs at the maximum test concentration (20 μM), which was evaluated using the Cell Counting Kit-8 (CCK-8) assay.[43]

With respect to structure−activity relationships, the experimental observations suggest the important role of stereochemistry, as exemplified by the two pairs of diastereoisomers. Compounds **2** and **8** exhibited more potent osteoclast differentiation inhibitory activities than their corresponding diastereoisomers **1** and **7**, respectively, despite having the same planar structure. The sugar unit appears to be responsible for the good activity because compound **3** with β-D-xylopyranose is more active than compound **6**, which contains a β-D-apiofuranose at the same position of the same aglycone as **3**. Compounds **2** and **8** have been reported to stimulate osteoblast differentiation assessed by alkaline phosphatase activity.[44] In addition, it was hypothesized that *C*-glycosylated flavonoids may be better therapeutic candidates because of their stability over aglycone and *O*-glycosylated flavonoids.

Inhibitory Effects of Compound 8 on RANKL-Induced Gene Expression. To investigate the mechanism of action of flavonoids in inhibition of osteoclast differentiation, the inhibitory effects of compound **8** on the mRNA expression of transcription factor NFATc1 as well as osteoclast-specific genes were confirmed by real-time PCR analysis. NFATc1 is a master regulator involved in osteoclast formation,[45] and an osteoclast-associated receptor (OSCAR) was characterized as an important osteoimmunological mediator.[46] The dendritic cell-specific transmembrane protein (DC-STAMP) and cathepsin K (CTSK) are found to be involved in fusion and bone resorptive activity, respectively.[47] It was reported that RANKL induction of these osteoclast-specific genes can be attenuated by the inactivation of NFATc1. As shown in Figure 4, the mRNA expression level of NFATc1 was activated in RANKL-treated cells (control) during the 3 day RANKL-treatment period. In contrast, the transcriptional expression level of NFATc1 was significantly suppressed after addition of compound **8**. Similarly, the mRNA expression levels of OSCAR, DC-STAMP, and CTSK were significantly reduced. These observations indicated that the osteoclast differentiation inhibitory activity of compound **8** could be caused by the downregulation of NFATc1 expression.

Compound 8 Inhibited the RANKL-Induced Protein Expression of NFATc1. Western blotting analysis was performed to examine the effect of compound **8** on the expression of NFATc1. Consistent with the mRNA expression data, the translational expression level of NFATc1 was activated after RANKL treatment and increased in proportion to the reaction time, but pretreatment of compound **8** (20 μM) significantly attenuated the protein expression of NFATc1 (Figure 5). The result suggested that compound **8** inhibited osteoclast formation by suppression of NFATc1 expression.

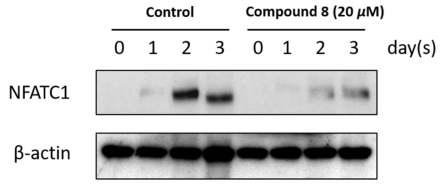

Figure 5. Effects of compound **8** (20 μM) on the RANKL-induced mediated protein expression of NFATc1. The expression of NFATc1 protein was evaluated by western blotting analysis after treatment with RANKL (10 ng/mL) and M-CSF (30 ng/mL) for 1, 2, and 3 days. Control: DMSO.

https://doi.org/10.1021/acsomega.1c05305
ACS Omega 2022, 7, 4840−4849

To the best of our knowledge, this is the first report of compounds **1**−**8** from *U. macrocarpa*. Detail NMR assignments were provided for all of the compounds including compounds **2**, **4**, and **7**, whose NMR data are not available in references despite recent isolation from *Clitoria guianensis*.[48] Compounds **2** and **8**, from a Western Himalayas species *U. wallichiana*,[44] were reported to stimulate osteoblast differentiation. The present study, for the first time, reported their inhibitory activities on RANKL-induced osteoclast differentiation. Both stimulation of osteoblast differentiation and inhibition of osteoclast differentiation are important for the treatment of osteopenic diseases because such diseases are mainly caused by the loss of balance between bone resorption by osteoclasts and bone formation by osteoblasts.[1]

In conclusion, the present study, for the first time, revealed (2*S*)-naringenin-6-*C*-*β*-D-glucopyranoside (**1**), (2*R*)-naringenin-6-*C*-*β*-D-glucopyranoside (**2**), (2*R*,3*S*)-catechin-7-*O*-*β*-D-xylopyranoside (**3**), (2*R*,3*S*)-catechin-7-*O*-*β*-D-apiofuranoside (**6**), (2*R*,3*R*)-taxifolin-6-*C*-*β*-D-glucopyranoside (**7**), and (2*S*,3*S*)-taxifolin-6-*C*-*β*-D-glucopyranoside (**8**) from *U. macrocarpa* Hance as osteoclast differentiation inhibitory constituents. Mechanistically, the compounds may exhibit osteoclast differentiation inhibitory activity via the downregulation of NFATc1, a master regulator involved in osteoclast formation. We hope that the present study will provide further scientific evidence for the rational application of the genus *Ulmus* in the treatment of osteopenic diseases such as osteoporosis.

■ ASSOCIATED CONTENT

Supporting Information

The Supporting Information is available free of charge at https://pubs.acs.org/doi/10.1021/acsomega.1c05305.

NMR (1D and 2D), LRMS and HRMS spectra of compounds **1**−**8**, and biological data of effects of compounds (**1**−**3**, **6**, and **7**) on RANKL-induced osteoclast differentiation (PDF)

■ AUTHOR INFORMATION

Corresponding Author

Heonjoong Kang − *Laboratory of Marine Drugs, School of Earth and Environmental Sciences, Seoul National University, Seoul 08826, Korea; Research Institute of Oceanography and Interdisciplinary Graduate Program in Genetic Engineering, Seoul National University, Seoul 08826, Korea; Bio-MAX Institute, Seoul National University, Seoul 08826, Korea;* orcid.org/0000-0001-5555-2898; Email: hjkang@snu.ac.kr

Authors

Weihong Wang − *Laboratory of Marine Drugs, School of Earth and Environmental Sciences, Seoul National University, Seoul 08826, Korea; Research Institute of Oceanography, Seoul National University, Seoul 08826, Korea*

Chanhyeok Jeong − *Department of Agricultural Biotechnology and Research Institute of Agriculture and Life Sciences, Seoul National University, Seoul 08826, Korea*

Yongjin Lee − *Department of Pharmacy, Sunchon National University, Suncheon, Jeollanam-do 57922, Korea*

Chanyoon Park − *Laboratory of Marine Drugs, School of Earth and Environmental Sciences, Seoul National University, Seoul 08826, Korea; Interdisciplinary Graduate Program in Genetic Engineering, Seoul National University, Seoul 08826, Korea*

Eunseok Oh − *Laboratory of Marine Drugs, School of Earth and Environmental Sciences, Seoul National University, Seoul 08826, Korea*

Kyu-Hyung Park − *Laboratory of Marine Drugs, School of Earth and Environmental Sciences, Seoul National University, Seoul 08826, Korea*

Youbin Cho − *Laboratory of Marine Drugs, School of Earth and Environmental Sciences, Seoul National University, Seoul 08826, Korea*

Eunmo Kang − *Laboratory of Marine Drugs, School of Earth and Environmental Sciences, Seoul National University, Seoul 08826, Korea*

JunI Lee − *Laboratory of Marine Drugs, School of Earth and Environmental Sciences, Seoul National University, Seoul 08826, Korea*

Yeon-Jin Cho − *Bio-MAX Institute, Seoul National University, Seoul 08826, Korea*

Jung Han Yoon Park − *Department of Agricultural Biotechnology and Research Institute of Agriculture and Life Sciences, Seoul National University, Seoul 08826, Korea; Advanced Institutes of Convergence Technology, Seoul National University, Suwon 16229, Korea*

Young-Jin Son − *Department of Pharmacy, Sunchon National University, Suncheon, Jeollanam-do 57922, Korea*

Ki Won Lee − *Department of Agricultural Biotechnology and Research Institute of Agriculture and Life Sciences and Bio-MAX Institute, Seoul National University, Seoul 08826, Korea; Advanced Institutes of Convergence Technology, Seoul National University, Suwon 16229, Korea*

Complete contact information is available at: https://pubs.acs.org/10.1021/acsomega.1c05305

Author Contributions

○W.W., C.J., and Y.L. contributed equally to this work.

Funding

This work was supported by the Basic Science Research Program funded by the Ministry of Science, ICT & Future Planning (2019R1A2C2005492) and by a service project from the Pyeongchang Revitalizing Program.

Notes

The authors declare no competing financial interest.

■ REFERENCES

(1) Boyle, W. J.; Simonet, W. S.; Lacey, D. L. Osteoclast differentiation and activation. *Nature* **2003**, *423*, 337−342.

(2) Xu, F.; Teitelbaum, S. L. Osteoclasts: New Insights. *Bone Res.* **2013**, *1*, 11−26.

(3) Charles, J. F.; Aliprantis, A. O. Osteoclasts: more than 'bone eaters'. *Trends Mol. Med.* **2014**, *20*, 449−459.

(4) Burden, A. M.; Tanaka, Y.; Xu, L.; Ha, Y. C.; McCloskey, E.; Cummings, S. R.; Gluer, C. C. Osteoporosis case ascertainment strategies in European and Asian countries: a comparative review. *Osteoporosis Int.* **2021**, *32*, 817−829.

(5) Zuo, L. H.; Shang, A. Q.; Zhang, S.; Yu, X. Y.; Ren, Y. C.; Yang, M. S.; Wang, J. M. The first complete chloroplast genome sequences of Ulmus species by de novo sequencing: Genome comparative and taxonomic position analysis. *PLoS One* **2017**, *12*, No. e0171264.

(6) Bate-Smith, E. C.; Richens, R. H. Flavonoid Chemistry and Taxonomy in Ulmus. *Biochem. Syst. Ecol.* **1973**, *1*, 141−146.

(7) Park, W. S. *Anatomical and Chemical Characterization of Ulmus Species from South Korea*; Gyeongsang National University, 2020.

(8) Lee, Y. N. *Plants in Korea*; Kyohak Co. Ltd.: Seoul, Korea, 2006.

(9) Park, J. H.; Kim, J. S. Chemical study on the root of *Ulmus macrocarpa*. *Korean J. Plant Resour.* **1994**, *7*, 103−108.
(10) So, H. M.; Yu, J. S.; Khan, Z.; Subedi, L.; Ko, Y.-J.; Lee, I. K.; Park, W. S.; Chung, S. J.; Ahn, M.-J.; Kim, S. Y.; Kim, K. H. Chemical constituents of the root bark of *Ulmus davidiana* var. japonica and their potential biological activities. *Bioorg. Chem.* **2019**, *91*, No. 103145.
(11) Kang, S. K.; Kim, K. S.; Byun, Y. S.; Suh, S. J.; Jim, U. H.; Kim, K. H.; Lee, I. S.; Kim, C. H. Effects of *Ulmus davidiana* planch on mineralization, bone morphogenetic protein-2, alkaline phosphatase, type I collagen, and collagenase-1 in bone cells. *In Vitro Cell. Dev. Biol.: Anim.* **2006**, *42*, 225−229.
(12) Seo, B. I.; Ju, Y. S.; Choi, H. Y.; Park; Roh, S. S.; Koo, J. S.; Kim, J. J.; Kim, D. Y. *Illustrated Book of Herbal Plants in Oriental Medicine*; DaeWondang: Korea, 2011; pp 353−357.
(13) Suh, S. J.; Yun, W. S.; Kim, K. S.; Jin, U. H.; Kim, J. K.; Kim, M. S.; Kwon, D. Y.; Kim, C. H. Stimulative effects of *Ulmus davidiana* Planch (Ulmaceae) on osteoblastic MC3T3-E1 cells. *J. Ethnopharmacol.* **2007**, *109*, 480−485.
(14) Kim, K. W.; Park, J. S.; Kim, K. S.; Jin, U. H.; Kim, J. K.; Suh, S. J.; Kim, C. H. Inhibition of *Ulmus davidiana* Planch (Ulmaceae) on bone resorption mediated by processing of cathepsin K in cultured mouse osteoclasts. *Phytother. Res.* **2008**, *22*, 511−517.
(15) Son, B. W.; Park, J. H.; Zee, O. P. Catechin Glycoside from *Ulmus davidiana*. *Arch. Pharmacal Res.* **1989**, *12*, 219−222.
(16) Lee, M. K.; Sung, S. H.; Lee, H. S.; Cho, J. H.; Kim, Y. C. Lignan and neolignan glycosides from *Ulmus davidiana* var. japonica. *Arch. Pharmacal Res.* **2001**, *24*, 198−201.
(17) Hosny, M.; Zheng, M.-S.; Zhang, H.; Chang, H.-W.; Woo, M.-H.; Son, J.-K.; Lee, S. K.-S. (-)-Catechin glycosides from *Ulmus davidiana*. *Arch. Pharmacal Res.* **2014**, *37*, 698−705.
(18) Ye, G.; Cao, Q.; Chen, X.; Li, S.; Jia, B. *Ulmus macrocarpa* hance for the treatment of ulcerative colitis–a report of 36 cases. *J. Tradit. Chin. Med.* **1990**, *10*, 97−98.
(19) Oh, K. S.; Ryu, S. Y.; Oh, B. K.; Seo, H. W.; Kim, Y. S.; Lee, B. H. Antihypertensive, vasorelaxant, and antioxidant effect of root bark of *Ulmus macrocarpa*. *Biol. Pharm. Bull.* **2008**, *31*, 2090−2096.
(20) Kwon, J.-H.; Kim, S.-B.; Park, K.-H.; Lee, M.-W. Antioxidative and anti-inflammatory effects of phenolic compounds from the roots of *Ulmus macrocarpa*. *Arch. Pharmacal Res.* **2011**, *34*, 1459−1466.
(21) Yang, W. K.; Lee, J. J.; Sung, Y. Y.; Kim, D. S.; Myung, C. S.; Kim, H. K. Extract of *Ulmus macrocarpa* Hance prevents thrombus formation through antiplatelet activity. *Mol. Med. Rep.* **2013**, *8*, 726−730.
(22) Choi, S. I.; Lee, J. H.; Kim, J. M.; Jung, T. D.; Cho, B. Y.; Choi, S. H.; Lee, D. W.; Kim, J.; Kim, J. Y.; Lee, O. H. *Ulmus macrocarpa* Hance Extracts Attenuated H(2)O(2) and UVB-Induced Skin Photo-Aging by Activating Antioxidant Enzymes and Inhibiting MAPK Pathways. *Int. J. Mol. Sci.* **2017**, *18*, No. 1200.
(23) Han, H. J.; Song, X.; Yadav, D.; Hwang, M. S.; Lee, J. H.; Lee, C. H.; Kim, T. H.; Lee, J. J.; Kwon, J. *Ulmus macrocarpa* Hance modulates lipid metabolism in hyperlipidemia via activation of AMPK pathway. *PLoS One* **2019**, *14*, No. e0217112.
(24) Rho, J.; Seo, C. S.; Park, H. S.; Wijerathne, C. U.; Jeong, H. Y.; Moon, O. S.; Seo, Y. W.; Son, H. Y.; Won, Y. S.; Kwun, H. J. *Ulmus macrocarpa* Hance improves benign prostatic hyperplasia by regulating prostatic cell apoptosis. *J. Ethnopharmacol.* **2019**, *233*, 115−122.
(25) Yeon, J. T.; Choi, S. W.; Ryu, B. J.; Kim, K. J.; Lee, J. Y.; Byun, B. J.; Son, Y. J.; Kim, S. H. Praeruptorin A Inhibits in Vitro Migration of Preosteoclasts and in Vivo Bone Erosion, Possibly Due to Its Potential To Target Calmodulin. *J. Nat. Prod.* **2015**, *78*, 776−782.
(26) Kim, K. J.; Lee, Y.; Son, S. R.; Lee, H.; Son, Y. J.; Lee, M. K.; Lee, M. Water Extracts of Hull-less Waxy Barley (*Hordeum vulgare* L.) Cultivar 'Boseokchal' Inhibit RANKL-induced Osteoclastogenesis. *Molecules* **2019**, *24*, No. 3735.
(27) Rozen, S.; Skaletsky, H. Primer3 on the WWW for general users and for biologist programmers. In *Methods in Molecular Biology*; Springer, 2000; Vol. *132*, pp 365−386.
(28) Altona, C.; Haasnoot, C. A. G. Prediction of Anti and Gauche Vicinal Proton-Proton Coupling-Constants in Carbohydrates - a Simple Additivity Rule for Pyranose Rings. *Org. Magn. Reson.* **1980**, *13*, 417−429.
(29) Stark, T.; Hofmann, T. Application of a molecular sensory science approach to alkalized cocoa (Theobroma cacao): Structure determination and sensory activity of nonenzymatically C-glycosylated flavan-3-ols. *J. Agric. Food Chem.* **2006**, *54*, 9510−9521.
(30) Stark, T.; Keller, D.; Wenker, K.; Hillmann, H.; Hofmann, T. Nonenzymatic C-glycosylation of flavan-3-ols by oligo- and polysaccharides. *J. Agric. Food Chem.* **2007**, *55*, 9685−9697.
(31) Gaffield, W. Circular Dichroism, Optical Rotatory Dispersion and Absolute Configuration of Flavanones, 3-Hydroxyflavanones and Their Glycosides - Determination of Aglycone Chirality in Flavanone Glycosides. *Tetrahedron* **1970**, *26*, 4093−4108.
(32) Snatzke, G. Circulardichroismus. 10. Modifizierung Der Octantenregel Fur Alpha,Beta-Ungesattigte Ketone - Cisoide Enone Dienone Und Arylketone. *Tetrahedron* **1965**, *21*, 439−448.
(33) Joo, S. J.; Park, H. J.; Park, J. H.; Cho, J. G.; Kang, J. H.; Jeong, T. S.; Kang, H. C.; Lee, D. Y.; Kim, H. S.; Byun, S. Y.; Baek, N. I. Flavonoids from *Machilus japonica* Stems and Their Inhibitory Effects on LDL Oxidation. *Int. J. Mol. Sci.* **2014**, *15*, 16418−16429.
(34) van Rensburg, H.; Steynberg, P. J.; Burger, J. F. W.; van Heerden, P. S.; Ferreira, D. Circular dichroic properties of flavan-3-ols. *J. Chem. Res.* **1999**, *23*, 450−451.
(35) Slade, D.; Ferreira, D.; Marais, J. P. J. Circular dichroism, a powerful tool for the assessment of absolute configuration of flavonoids. *Phytochemistry* **2005**, *66*, 2177−2215.
(36) Nel Reinier, J. J.; van Rensburg, H.; van Heerden, P. S.; Ferreira, D. Stereoselective synthesis of flavonoids. Part 8. Free phenolic flavan-3-ol diastereoisomers. *J. Chem. Res.* **1999**, *23*, 606−607.
(37) Cunha, C. L.; Siebeneichler, S. C.; Nascimento, I. R.; Holzbach, J. C. New isoflavone and other constituents from roots of *Clitoria guianensis*. *J. Braz. Chem. Soc.* **2020**, *31*, 1753−1757.
(38) Stark, T. D.; Ranner, J.; Stiglbauer, B.; Weiss, P.; Stark, S.; Balemba, O. B.; Hofmann, T. Construction and Application of a Database for a Five-Dimensional Identification of Natural Compounds in Garcinia Species by Means of UPLC-ESI-TWIMS-TOF-MS: Introducing Gas Phase Polyphenol Conformer Drift Time Distribution Intensity Ratios. *J. Agric. Food Chem.* **2019**, *67*, 975−985.
(39) Kruk, J.; Baranowska, I.; Buszewski, B.; Bajkacz, S.; Kowalski, B.; Ligor, M. Flavonoids enantiomer distribution in different parts of goldenrod (*Solidago virgaurea* L.), lucerne (*Medicago sativa* L.) and phacelia (*Phacelia tanacetifolia* Benth.). *Chirality* **2019**, *31*, 138−149.
(40) Rinaldo, D.; Batista, J. M.; Rodrigues, J.; Benfatti, A. C.; Rodrigues, C. M.; Dos Santos, L. C.; Furlan, M.; Vilegas, W. Determination of Catechin Diastereomers from the Leaves of Byrsonima species Using Chiral HPLC-PAD-CD. *Chirality* **2010**, *22*, 726−733.
(41) Ikeda, K.; Takeshita, S. The role of osteoclast differentiation and function in skeletal homeostasis. *J. Biochem.* **2016**, *159*, 1−8.
(42) Asagiri, M.; Takayanagi, H. The molecular understanding of osteoclast differentiation. *Bone* **2007**, *40*, 251−264.
(43) Tominaga, H.; Ishiyama, M.; Ohseto, F.; Sasamoto, K.; Hamamoto, T.; Suzuki, K.; Watanabe, M. A water-soluble tetrazolium salt useful for colorimetric cell viability assay. *Anal. Commun.* **1999**, *36*, 47−50.
(44) Rawat, P.; Kumar, M.; Sharan, K.; Chattopadhyay, N.; Maurya, R. Ulmosides A and B: Flavonoid 6-C-glycosides from *Ulmus wallichiana*, stimulating osteoblast differentiation assessed by alkaline phosphatase. *Bioorg. Med. Chem. Lett.* **2009**, *19*, 4684−4687.
(45) Takayanagi, H. Osteoimmunology: shared mechanisms and crosstalk between the immune and bone systems. *Nat. Rev. Immunol.* **2007**, *7*, 292−304.
(46) Nemeth, K.; Schoppet, M.; Al-Fakhri, N.; Helas, S.; Jessberger, R.; Hofbauer, L. C.; Goettsch, C. The Role of Osteoclast-Associated Receptor in Osteoimmunology. *J. Immunol.* **2011**, *186*, 13−18.

https://doi.org/10.1021/acsomega.1c05305
ACS Omega 2022, 7, 4840−4849

(47) Yagi, M.; Miyamoto, T.; Sawatani, Y.; Iwamoto, K.; Hosogane, N.; Fujita, N.; Morita, K.; Ninomiya, K.; Suzuki, T.; Miyamoto, K.; Oike, Y.; Takeya, M.; Toyama, Y.; Suda, T. DC-STAMP is essential for cell-cell fusion in osteoclasts and foreign body giant cells. *J. Exp. Med.* **2005**, *202*, 345−351.
(48) Cunha, C. L.; Siebeneichler, S. C.; Nascimento, I. R.; Holzbach, J. C. A New Isoflavone and Other Constituents from Roots of *Clitoria guianensis*. *J. Braz. Chem. Soc.* **2020**, *31*, 1753−1757.

https://doi.org/10.1021/acsomega.1c05305
ACS Omega 2022, 7, 4840−4849